Abdelkader BOUDALI[1], Karim NEGADI[1], Mohamed BOUDIAF[2], Abderrahmane BERKANI[1], Fabrizio MARIGNETTI[3]

Laboratory of L2GEGI, Department of Electrical Engineering, University of Tiaret, Algeria (1)
Department of Electrical Engineering, University Ziane Achour of Djelfa, Algeria (2)
Dipartimento di Automazione Università degli Studi di Cassino, Italy (3)

doi:10.15199/48.2020.10.25

Super Twisting Sliding Mode Controller of Small Hydropower Plant Energy Generation based DFIG

Abstract. *This paper presents the modeling, control, simulation and analysis of the dynamic small hydropower plant connected to the grid. Studied system comprises a small hydropower, a double fed induction generator (DFIG), and two converters linked by a DC bus. The whole is connected to the grid through a resistor–inductor filter. Hence, this paper proposed and discusses an efficient design based on a Super Twisting Sliding Mode Control (STSMC) applied side generator and side grid. The considered control of hydropower plant system was implemented in the Matlab/Simulink, the results show the effectiveness of the proposed method. The prototype simulated can be realized in an experimental test bench based FPGA, DSP or Dspace controller board.*

Streszczenie. *W pracy przedstawiono modelowanie, sterowanie, symulację i analizę dynamicznej małej elektrowni wodnej podłączonej do sieci. Badany system składa się z podwójnie zasilanego generatora indukcyjnego (DFIG) i dwóch przetworników połączonych szyną prądu stałego. Całość jest podłączona do sieci za pomocą filtru RC. W związku z tym w niniejszym artykule zaproponowano i omówiono skuteczną konstrukcję opartą na zastosowanym generatorze bocznym Super Twisting Sliding Mode Control i STSMC. Styerowaniesystemem elektrowni wodnych zostało zbadane w Matlab/ Simulink. Wyniki pokazują skuteczność proponowanej metody. Symulowany prototyp można zrealizować w eksperymentalnej płycie kontrolnej opartej na FPGA, DSP lub Dspace.* ***Sterowanie typu Super Twisting Sliding małej elektrowni wodnej z generatorem D****FIG*

Keywords: Small hydropower plant, DFIG, Vienna rectifier, Super Twisting Sliding Mode Controller (STSMC), Power generation,.
Słowa kluczowe: Mała elektrownia wodna, DFIG, prostownik wiedeński, sterownik SuperSkręcanego Trybu Przesuwnego (STSMC).

Introduction

Small hydro power plants are widely used more and more in the context of renewable energy [1]. Large applications to small hydroelectric power plants (SHPP) even in countries with few water resources have shown that variable speed operations can gain more hydraulic power than the fixed speed case [1, 2]. Besides, variable speed techniques can improve the operation process such as mitigating the cavitations effects, alleviating water hammer disturbances, and optimizing transient processes. Due to the benefits of variable speed operation, large efforts have been contributed.

Numerous analytical and practical studies and research have been interested in determining the model of small hydroelectric power stations (SHPP). The general structures of large-scale HPPs and SHPPs are basically the same. Therefore, previous studies employed models of large-scale HPPs in the modeling of SHPPs [3].

However, the hydroelectric power system presents a complexity due to the high non-linearity which generates uncertainties, turbulence in the speed of hydroelectricity and changes in the parameters of the hydroelectric system. Non-linear control strategies have been implemented, to deal with the problem of non-linearity.

Therefore, there are a lot of intelligent nonlinear techniques used to overcome this difficulty, such as fuzzy logic and neural network. In addition, sliding mode control (SMC) approach can be used. It has a good performance because of the insensitivity to external disturbance and to the nonlinearity of system. Several researchers developed a control strategy based on a controller by Super Twisting sliding mode (STSM) [4, 5]. The chattering phenomenon is the major drawback of practical implementation of this strategy. To address this problem, a control strategy by sliding mode of higher order was implemented on the basis of the super-twisting algorithm.

This work is structured according to the following plan: in section 2, the model of the hydraulic turbine is defined. The system configuration and the models of components employed for each subsystem are described in section 4. Physical modeling of the DFIG and the Vienne rectifier with their equations model is shown in section 3 and 4. In section 5 and 6, the STSM control is presented on rotor and grid side converter. Section 7 validated the theoretical study part and the proposed control algorithms implemented and a dynamic model of the system is modeled and simulated in Matlab / Simulink. Finally, conclusions are drawn in section 8.

Model of the hydraulic turbine

The MHPP operation principle consists of transforming the hydraulic energy into electrical energy. Through a water tunnel, the water reaches a surge tank that supplies a penstock characterized by its height.

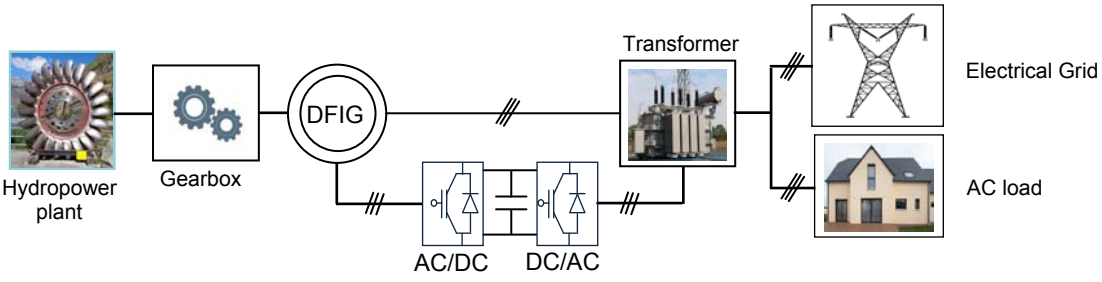

Fig. 1. Main components of hydropower plant

At the output of this latter, the water rotates a hydraulic turbine which drives a synchronous generator. The generator produces electricity that feeds loads which can be composed from three or/and single-phase loads. Fig. 1 shows the various components of the constituting hydropower plants.

The power absorbed from the hydraulic turbine depends on the net water head – H [m] and the water flow rate – Q_ω [m^3/s] [6]:

$$p_h = \rho g H Q_\omega \tag{1}$$

Hydraulic turbine efficiency: – η is defined as the ratio of mechanical power transmitted by the shaft to the absorbed hydraulic power, which strongly affects the net output mechanical power P_m [Watt]:

$$p_m = \eta \rho g H Q_\omega \tag{2}$$

where: – ρ [kg.m^3] is the volume density of water, *a*: – the acceleration due to gravity [m.s^{-2}].
The mechanical torque could be given by:

$$T_m = \frac{P_m}{\omega} \tag{3}$$

where: – ω [rad.s^{-1}] represents the turbine rotation speed.

According to equations of turbine model, the plot of the hydraulic turbine characteristics is shown in Fig. 2. This plot is in function according to several values of mechanical and speed turbine.

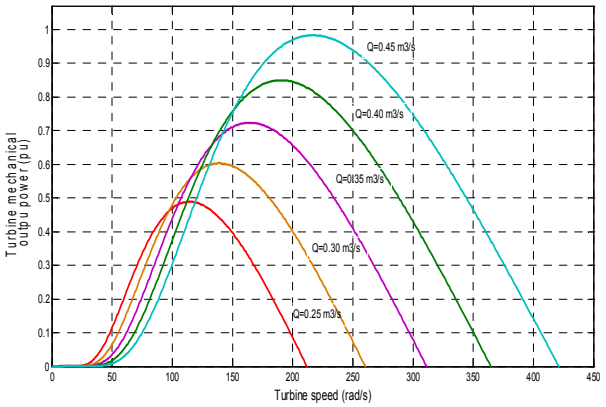

Fig. 2. Hydraulic turbine characteristic

Mathematic model of Double Fed Induction Generator

The electrical model of the DFIG in the d-q frame linked to the stator rotating field is given by the system [7]:

$$\begin{cases} v_{sd} = R_s i_{sd} + \dfrac{d\psi_{sd}}{dt} - \omega_s i_{sq} \\ v_{sq} = R_s i_{sq} + \dfrac{d\psi_{sq}}{dt} + \omega_s i_{sd} \\ v_{rd} = R_r i_{rd} + \dfrac{d\psi_{rd}}{dt} - \omega_r i_{rq} \\ v_{rq} = R_r i_{sq} + \dfrac{d\psi_{rq}}{dt} + \omega_r i_{rd} \end{cases} \tag{4}$$

where:

$$\begin{cases} \psi_{sd} = L_s i_{sd} + M i_{rd} \\ \psi_{sq} = L_s i_{sq} + M i_{rq} \\ \psi_{rd} = L_r i_{rd} + M i_{sd} \\ \psi_{rq} = L_r i_{rq} + M i_{sq} \end{cases} \tag{5}$$

The electromagnetic torque is given by:

$$T_{em} = pM\left(i_{rd} i_{sq} - i_{rq} i_{sd}\right) \tag{6}$$

Vienna rectifier topology

The Vienna rectifier is an advantageous unidirectional PFC (power factor correction) rectifier with less number of active power switches, sinusoidal input current, and balanced output DC-link voltage, low voltage stress across switches, high switching operation and high efficiency [8].

The boost type rectifier is used for the wind, micro turbines, low voltage DC (LVDC), high voltage DC distribution (HVDC) and AC mains at the front side for higher voltages of 400V-750V-1500V.

As Fig. 3 shown, it consists of 3- switches and 18-diodes with DC-link capacitor at the output. The current flows through the three MOSETs and the capacitors in the fully charged it.

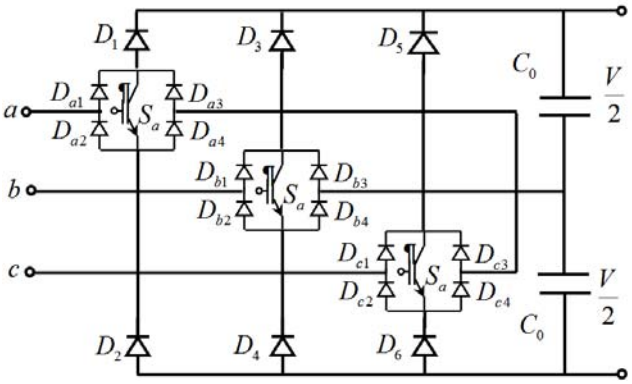

Fig. 3. Topology of power Vienna rectifier

The phase current rises, through a MOSFETs, during that pulse period, charge the capacitor. When the MOSFETs is turned off, current through the diode upper or lower depending on direction of the current flow. By adjust the width of the pulse that turns ON the MOSFETs, corresponding line current is forced to be sinusoidal and in phase with the Voltage. When the MOSFETs is turned ON the corresponding phase is connected the line inductor, to the center point between the two output capacitors.

Control of the rotor side converter (RSC)

The DFIG-based hydraulic turbine control objective is to optimize the hydraulic energy capture by tracking the optimal torque T^* [9].

For these purposes, let us consider the tracking errors

$$\begin{cases} s_1 = i_{rd} - i_{rd}^* \\ s_2 = T_{em} - T_{em}^* \end{cases} \tag{7}$$

Then we will have:

(8)

$$\begin{cases} \dot{s}_1 = \dfrac{1}{\sigma L_r}\left(v_{rd} - R_r i_{rd} + s\omega_s \sigma L_r i_{rq} - \dfrac{M}{L_s}\dfrac{d\psi_{sd}}{dt} \right) - i_{rd}^* \\ \dot{s}_2 = -\dfrac{pM}{\sigma L_s L_r}\psi_{sd}\left(v_{rq} - R_r i_{rq} - s\omega_s \sigma L_r i_{rd} - s\omega_s \dfrac{M}{L_s}\psi_{sd} \right) - T_{em}^* \end{cases}$$

We define the functions H_1 and H_2 as follows:

(9)

$$\begin{cases} H_1 = \dfrac{1}{\sigma L_r}\left(-R_r i_{rd} + s\omega_s \sigma L_r i_{rq} - \dfrac{M}{L_s}\dfrac{d\psi_{sd}}{dt} \right) - i_{rd}^* \\ H_2 = -\dfrac{pM}{\sigma L_s L_r}\psi_{sd}\left(-R_r i_{rq} - s\omega_s \sigma L_r i_{rd} - s\omega_s \dfrac{M}{L_s}\psi_{sd} \right) - T_{em}^* \end{cases}$$

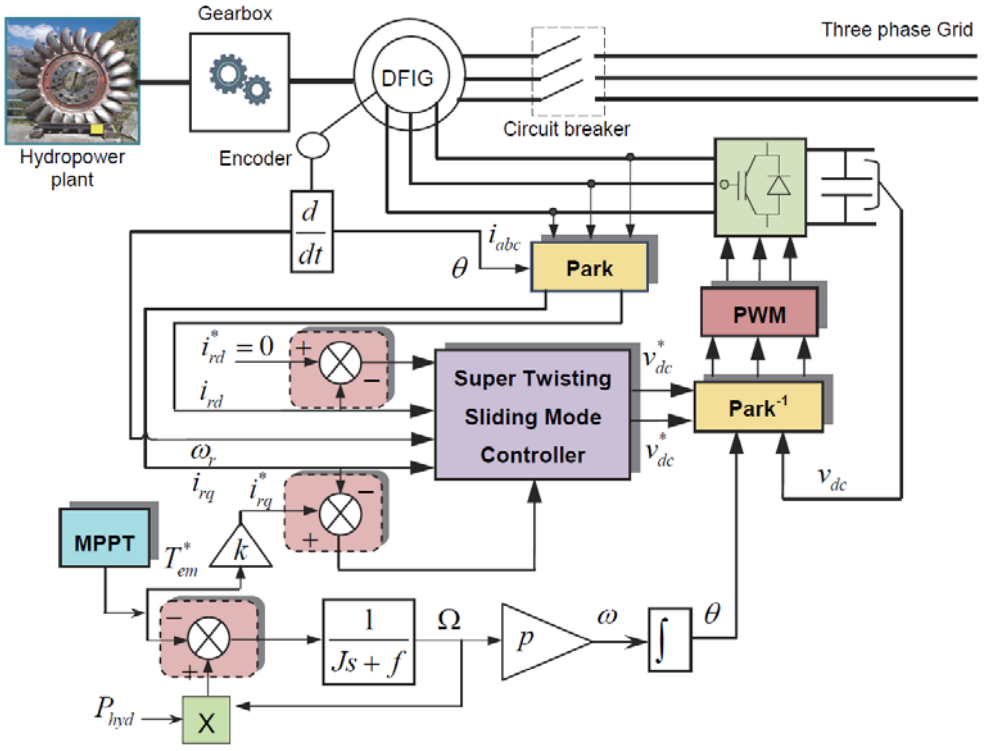

Fig. 4. STSM control of the rotor side converter

The second derivative of sliding surfaces is given by the following equation:

(10)

$$\begin{cases} \ddot{s}_1 = \dfrac{1}{\sigma L_r}\dot{v}_{rd} + \dot{H}_1 \\ \ddot{s}_2 = -\dfrac{pM}{\sigma L_s L_r}\dot{v}_{rq}\psi_s + \dot{H}_2 \end{cases}$$

where:

$$\begin{cases} v_{rd} = y_1 + \eta_1\sqrt{|s_2|} + sign(s_2) \\ v_{rq} = y_2 + \eta_2\sqrt{|s_1|} + sign(s_1) \end{cases},$$

and:

$$\begin{cases} \dot{y}_1 = \eta_3 sign(s_1) \\ \dot{y}_2 = -\eta_4 sign(s_2) \end{cases}$$

where: η_1, η_2, η_3 and η_4 are a constants that satisfactory the follows conditions [10]:

$$\begin{cases} \sigma_1 > \dfrac{\psi_2}{\sigma L_r} \\ \sigma_3 > \dfrac{pM}{\sigma L_s L_r}\psi_1 \end{cases}$$

and:

$$\begin{cases} \sigma_2^2 \geq \dfrac{4\psi_1(\eta_1 + \psi_1)}{\sigma^2 L_r^2(\eta_1 - \psi_1)} \\ \sigma_4^2 \geq \dfrac{4\psi_2(\eta_3 + \psi_2)}{\sigma^2 L_r^2(\eta_3 - \psi_2)} \end{cases}$$

and:

$$\begin{cases} |\dot{H}_1| < \psi_1 \\ |\dot{H}_2| < \psi_2 \end{cases}$$

Then the DFIG control strategy after connecting to the grid is as shown in Fig. 4.

Control of the grid side converter (GSC)

The i_{dg}^*, i_{qg}^* currents references are linked to the desirable active and reactive grid powers are derived as follows [11]:

(11)

$$\begin{cases} i_{dg}^* = \dfrac{P_g^*}{1.5 v_{gd}} \\ i_{qg}^* = \dfrac{Q_g^*}{1.5 v_{gd}} \end{cases}$$

The optimal reactive power is set to zero to ensure a unity power factor operation of this system: $Q^* = 0$,

whereas the optimal active power P^* can be written depending on the needs of the grid. The schematic diagram of the SOSMC applied to the grid side converter is illustrated in Fig. 5 [12].

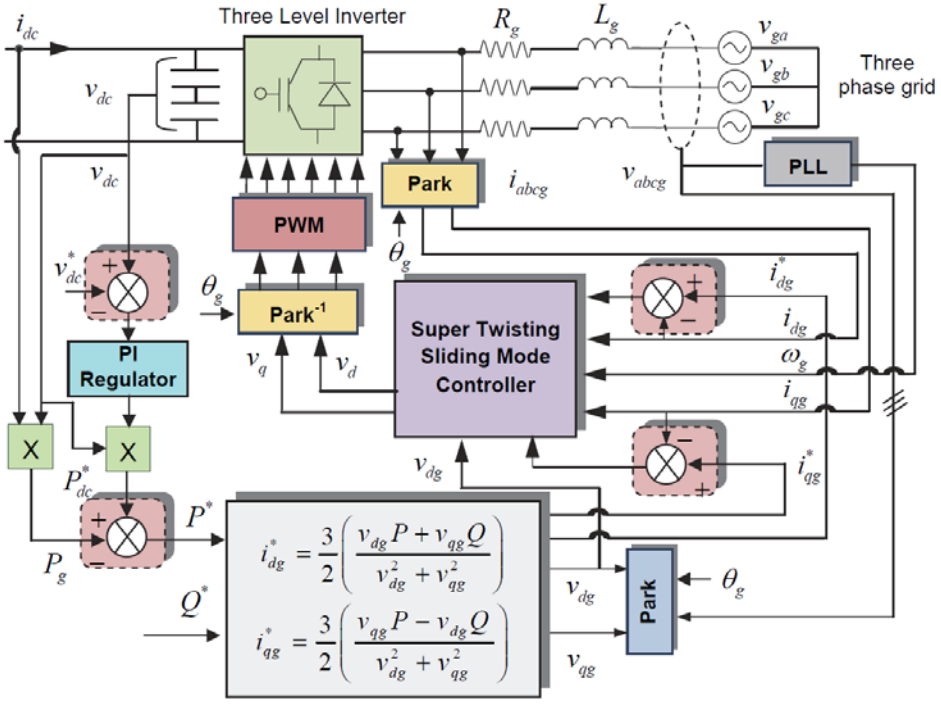

Fig. 5. STSM Control of grid side converter

After the first derivation of the both surfaces: Then we will have:

$$(13)\qquad \begin{cases} \dot{s}_d = \dot{i}_{dg}^* + \dfrac{1}{L_g}\left(v_{dg} + R_g i_{dg} - L_g \omega_g i_{qg}\right) - \dfrac{v_{di}}{L_g} \\ \dot{s}_q = \dot{i}_{qg}^* + \dfrac{1}{L_g}\left(v_{qg} + R_g i_{qg} + L_g \omega_g i_{dg}\right) - \dfrac{v_{di}}{L_g} \end{cases}$$

If we define the functions and H_d and H_q as follows:

$$(14)\qquad \begin{cases} H_d = \dot{i}_{dg}^* + \dfrac{1}{L_g}\left(v_{dg} + R_g i_{dg} - L_g \omega_g i_{qg}\right) \\ H_q = \dot{i}_{qg}^* + \dfrac{1}{L_g}\left(v_{qg} + R_g i_{qg} + L_g \omega_g i_{dg}\right) \end{cases}$$

The second derivative of sliding surfaces is given by the following equation [13, 14]:

$$(15)\qquad \begin{cases} \ddot{s}_d = \dot{H}_d - \dfrac{\dot{v}_{di}}{L_g} \\ \ddot{s}_q = \dot{H}_q - \dfrac{\dot{v}_{qi}}{L_g} \end{cases}$$

The control algorithm proposed which is based on super twisting algorithm (ST) two parts [11]:

$$(16)\qquad \begin{cases} v_{di}^* = v_{dieq} + v_{diN} \\ v_{qi}^* = v_{qieq} + v_{qiN} \end{cases}$$

with:

Let us introduce the following sliding surface for the direct and quadrature current i_{dg}, i_{qg}, respectively.

$$(12)\qquad \begin{cases} s_d = i_{dg}^* - i_{dg} \\ s_q = i_{qg}^* - i_{qg} \end{cases}$$

$$\begin{cases} v_{diN} = u_1 + u_2 \\ v_{qiN} = \sigma_1 + \sigma_2 \end{cases}$$

where:

$$\begin{cases} \dot{u}_1 = -k_1 \mathrm{sign}\left(s_d\right) \\ u_2 = M_1 \sqrt{\left|s_d\right|}\,\mathrm{sign}\left(s_d\right) \end{cases}$$

and:

$$\begin{cases} \dot{\sigma}_1 = -k_2 \mathrm{sign}\left(s_q\right) \\ \sigma_2 = M_2 \sqrt{\left|s_q\right|}\,\mathrm{sign}\left(s_q\right) \end{cases}$$

Simulation results and discussions

Simulations were carried out under the Matlab/Simulink platform for a 2 MW DFIG with the characteristics shown in Table 1 and the frequency of the AC grid was 50 Hz (characteristics of the DC-AC converter and the grid illustrated in Table 2).

The amount of power generated/supplied by the hydroelectric turbine depends on the variable water flow rated Q = 0.9 m^3/s at the time between t= [1-5 s], Q = 0.7 m^3/s at the time between t= [20.5-25 s] and Q = 0.5 m^3/s at the time between t= [25.5-30 s] respectively (Fig. 6 (a)).

As the water flow changes, Fig. 6 (b) show that the mechanical torque ripple is smaller. The synchronous speed of the rotor display in Fig. 6 (c) was 1 pu. The mechanical speed of the generator follows the reference that is determined by control strategy to capture the maximum hydroelectric power. The mechanical speed has a faster response.

Figure 7 (a) and (b) displayed respectively the three phase stator voltage and current and its zoom. It seen that these curves are purely sinusoidal and are affected by the instants of variations. Before t=6 s, generator current equal zero because the break is open so the generator is disconnect from the grid. Fig. 8 (a), (b) displayed in pu respectively the electromagnetic torque and the d, q components of the rotor voltage and current. These results present less chattering and respond appropriately to the proposed variation.

Figure 8 and 9 shows that the electromagnetic torque and the rotor flux component ripple using the high order sliding mode controller method is smaller. Both parts of the figure show average amplitude of the rotor flux around 1 pu.

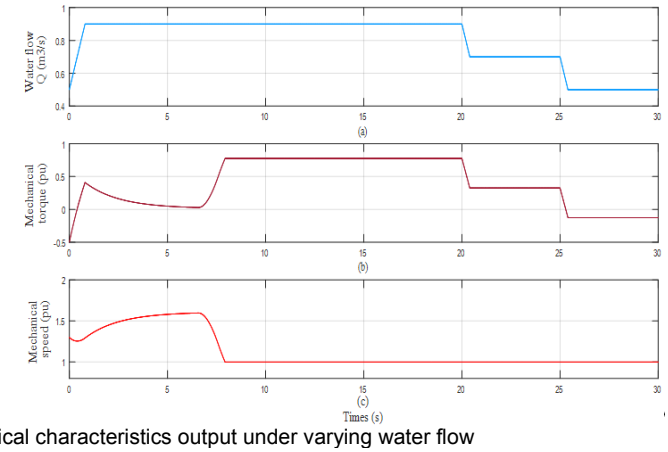

Fig. 6. Hydropower plant mechanical characteristics output under varying water flow

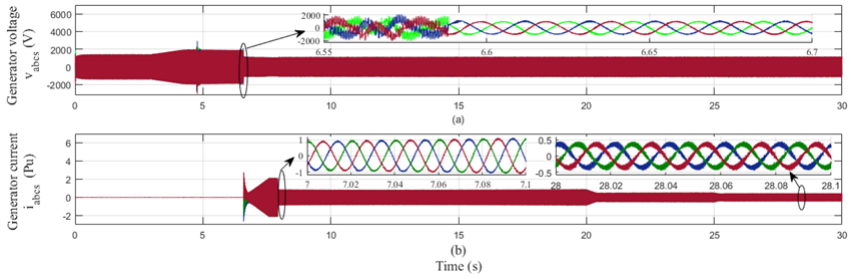

Fig. 7. Hydropower plant generator output voltage and current under varying water flow

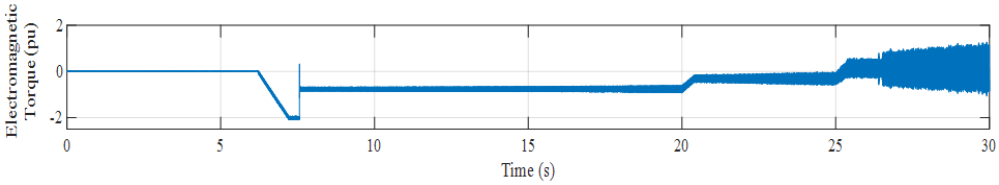

Fig. 8. Electromagnetic torque response of the DFIG using the proposed control strategy

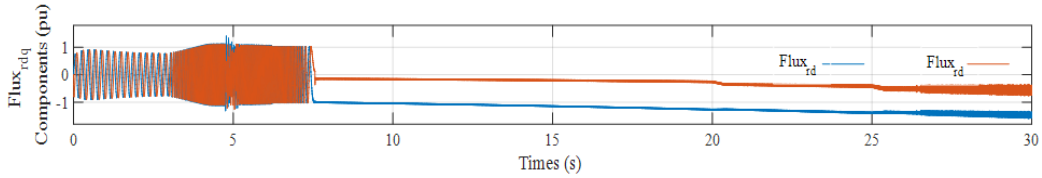

Fig. 9. Tracking performance obtained: rotor flux d, q components of the DFIG

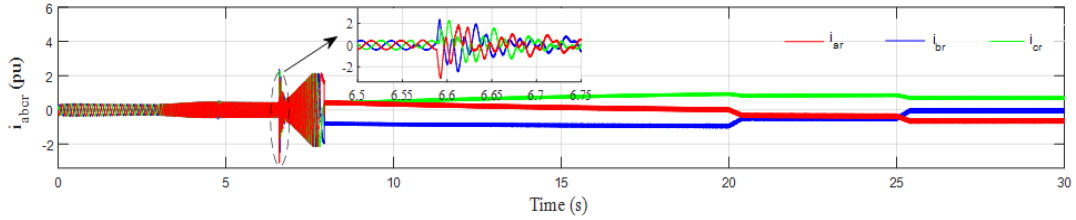

Fig. 10. Tracking performance obtained: three phase rotor current response of the DFIG

The maximum deviation of the rotor flux in Fig. 9 is 0.15 pu. That means the DFIG system using the STSMC method has reduced the deviation of the rotor flux by 44.4%.

Figure 10 shows the three phase rotor current of the DFIG in pu and its zoom.

These currents are sinusoidal until the instant of 8 seconds, after this period these currents have a behavior which makes it possible to respond to the proposed variations and make it possible to connect our studied conversion chain to the grid. One important performance measure of a DFIG system is the voltage of DC-link between the rotor-side converter and the grid-side converter, as shown is Fig. 11. The DC bus voltage, the generator and the grid frequency responses with STSM controller remain outstandingly insensible to the variation of the hydraulic water flow with smaller ripple.

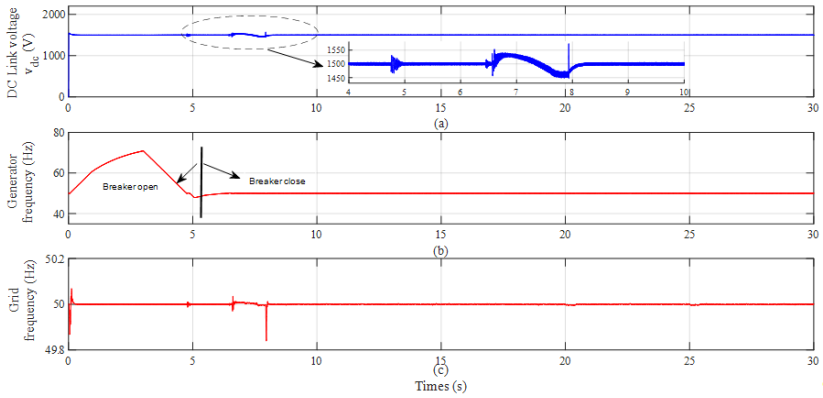

Fig. 11. Tracking performance of proposed control: (a) dc link voltage, (b) generator frequency and (c) grid frequency

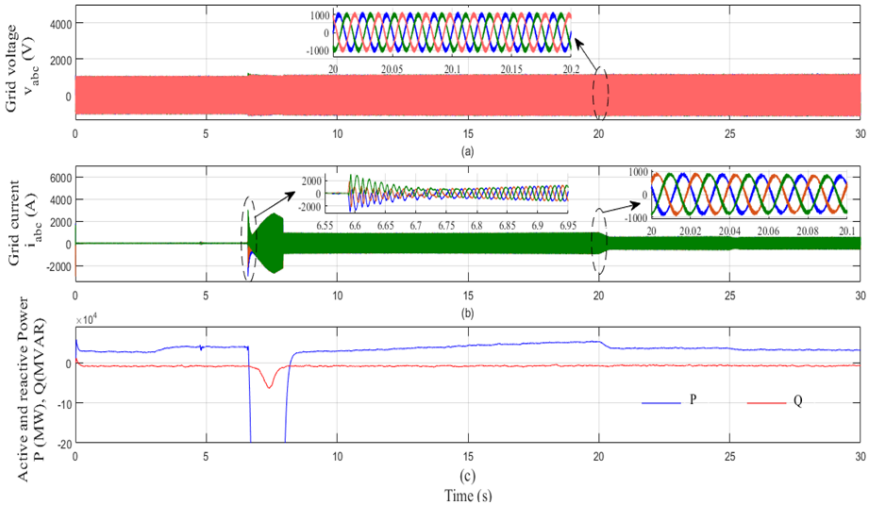

Fig. 12. Tracking performance of the proposed control strategy: (a) grid voltage, (b) grid current and (c) active and reactive powers

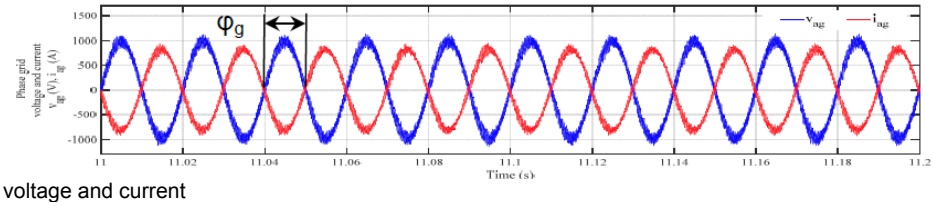

Fig. 13. Phase grid voltage and current

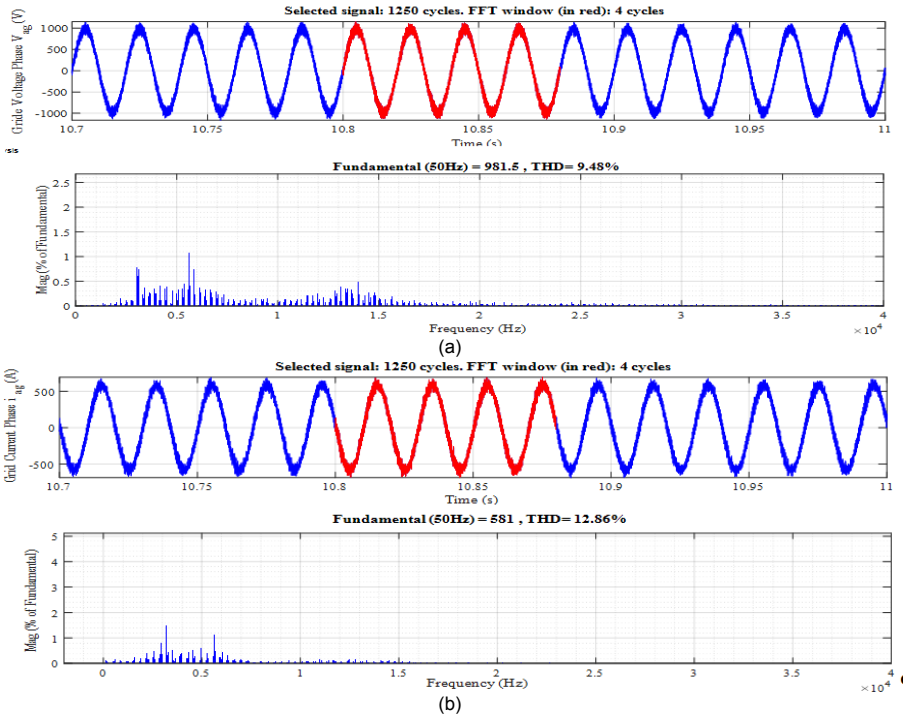

Fig. 14. THD and spectrum analysis: (a) grid voltage, (b) grid current

This is due its high ability to reject the disturbances and uncertainties, ST algorithm do not depend on the system parameters, such as that the highest robustness can be achieved. The Fig. 12 (a) and (b) respectively show the current and the voltage of the grid with their zoom, they are purely sinusoidal which shows the efficiency of the control strategy applied to the converter which gives a better quality of energy to the grid and the load. Fig. 12 (c) show the variations of active and reactive power, the active power keeps its nominal value of 2 MW and the reactive power remains near zero MVAR with slight disturbances appear at the instants of variations in water flow and with fast response time. Fig. 13 shows the grid phase A voltage and current, we notice that these quantities are 180° degree phase shift which means the reactive power equal to zero.

Figure 14 (a) and (b) illustrates respectively a sample waveform of the grid voltage and current for phase A. To see the efficiency of the proposed control strategy, a harmonic frequency spectrum estimated by means of a FFT analysis and total harmonic distortion (THD) of the grid current and voltage are show in Fig. 14 where each harmonic amplitude is expressed in percentage of the amplitude of the fundamental. THD is about 9.48 % and 12.86 % respectively.

Extensive simulations under different working conditions are performed for the considered hydroelectric dynamic process. The achieved results indicate that the proposed methodology is effective to accurately describe the hydroelectric power plant nonlinear dynamics as well as to design a hydraulic turbine speed control system.

8. Conclusions

A nonlinear control for a grid-connected hydroelectric power plant energy based DFIG connected directly to the grid by the stator and fed by a Vienne rectifier and three level converters on the rotor side has been presented in this article. The main objective was the implementation of a STSMC technique of stator active and reactive powers generated by the stator side of the DFIG in order to make the system insensible with the external disturbance. On the other hand, the proposed approach use in the conversion chain compared with conventional modulation technique gives a minimum THD value and powers ripples and it considerably reduces chatter active power and electromagnetic torque, avoiding the damage of excessive mechanical stress hydroelectric turbine.

As future work, the proposed methods may also be employed for preliminary designs or assessments of hydropower projects and can be implemented easily with FPGA, DSP or Dspace controller board platform.

APPENDIX

Table 1. DFIG parameters

Components	Rating values
Rated power	1600 kVA
Rated voltage Vrms	1200 V
Stator and rotor resistance	0.01379, 0.007728 pu
Stator, rotor and mutual inductance	0.0955, 0.0955, 2.416 pu
Inertia constant	1.1 pu
Friction factor	0.008726 pu
Pole pairs	2

Table 2. DC-AC inverter and grid parameters

Components	Rating values
Rated current	1000 A
Frequency	50 Hz
Rated voltage Vrms	1200 V
Capacity rating	0.01 F

Nomenclature

v_{dg}, v_{gg} – grid peak voltages in dq frame [V]
v_{sd}, v_{sq} – the d, q components of the stator voltage
v_{rd}, v_{rq} - the d, q components of the rotor voltage
v_{id}, v_{iq} - voltage inverter d, q componednts p[V]
i_{dg}, i_{qg} – grid peak currents in dq frame [A]
i_{sd}, i_{sq} – the d, q components of the stator current
i_{rd}, i_{rq} – the d, q components of the rotor current
Ψ_{sd}, Ψ_{sq} – the d, q components of the stator flux
Ψ_{rd}, Ψ_{rq} – the d, q components of the rotor flux
R_s, R_r – the stator and rotor resistance
L_s, L_r – the stator and rotor inductance
M – the magnetizing inductance
g – slip of DFIG
ω_s, ω_r – the synchronous rotor angular speed
$\omega_{sl=}\omega_s$-ω_r – the slip angular speed
R_g – input filter resistance [Ω]
L_{dg}, L_{qg} – input filter inductance d, q components [mH]
ω_g – grid angular frequency [rad/s]
v_{dc} – DC bus voltage [V]
v^*_{dc} – reference DC bus voltage [V]
i_{dc} – DC bus current [A]
C – DC link capacitor [mF]
R_s – load resistance [Ω]
P_g – grid active power [kW]
P^*_g - – grid active power reference[kW]
P_c – the power in capacitor
P_g – grid active power
P_r – the the active power at rotor side converter
P_m – the mechanical power
P – number of pole pairs in a generator
Q_g – grid reactive power [kVAR]
Q^*_g grid reactive power reference [kVAR]
Q_ω - water flow [m^3/s]
S_{ai} – switching state
T_{em} – electromagnetic torque [Nm]
T_m – the mechanical torque [Nm]
T_s – sampling time [μs]
f – grid frequency [Hz]
k – present sampling instant discrete-time frame
$k+1$ - future sampling instant discrete-time frame
k-1 – past sampling instant discrete-time frame
H – water heat
φ_g – grid power factor angle (angle between grid voltage and current [deg])
η - hydraulic turbine efficiency
ρ - the volume density of water [kg m^{-3}]
α - the acceleration due to gravity [m s^{-2}]
ω - the turbine rotation speed [rad/s]
AC - Alternatif Current
DC - Direct Current
DFIG - Double Fed Induction Generator
DSP - Digital Signal Processor
FPGA - Field Programmable Gate Arrays
GSC - Grid Side Converter
HPP - HydroPower Plant
HVDC - High Voltage Direct Current
LVDC - Low Voltage Direct Current
MOSFET - Metal Oxide Semiconductor Field Effect Transistor
NPC - Neutral Point Clamped
PI - Proportionnal Intergal
PPC - Predictive Power Control
Pu - Pert Unit
PWM - Pulse Width Modulation
RCS - Rotor Side Converter
STSMC Super Twistin Sliding Mode Control

Authors *Abdelkader Boudali, Laboratory of Energy and Computer Engineering L2GEGI, Department of Electrical Engineering, Faculty of Applied Sciences, University of Tiaret, BP 78 Size Zarroura, Tiaret 14000, Algeria, abdelkader.boudali@univ-tiaret.dz*
Karim Negadi, Laboratory of Energy and Computer Engineering L2GEGI, Department of Electrical Engineering, Faculty of Applied Sciences, University of Tiaret, BP 78 Size Zarroura, Tiaret 14000, Algeria, karim.negadi@univ-tiaret.dz
Mohamed Boudiaf, Department of Electrical Engineering, University Ziane Achour of Djelfa, Algeria, boudhiaf_mohamed@yahoo.fr
Abderrahmane Berkani, Laboratory of Energy and Computer Engineering L2GEGI, Department of Electrical Engineering, Faculty of Applied Sciences, University of Tiaret, BP 78 Size Zarroura, Tiaret 14000, Algeria, abderrahmane.berkani@univ-tiaret.dz
Fabrizio Marignetti, Dipartimento di Automazione Università degli Studi di Cassino*, Italy, marignetti@unicas.it*

REFERENCES

[1] Baoling G., Bacha S., Alamir M., Amgad M., Variable speed micro-hydro power generation system: Review and Experimental results, Symposium de Génie Electrique (SGE 2018), 3-5 Juillet 2018, Nancy, France.
[2] Weijia Yang., Dynamic Processes and Active Power Control of Hydropower Plants, Thesis Uppsala University, May 2017.
[3] Guan Y., Quintero J. C. V., Guerrero J. M., Wang Y., & Feng W., Frequency Stability of Hierarchically Controlled Hybrid Photovoltaic-Battery-Hydropower Microgrids, I E E E Transactions on Industry Applications, 51(6), 4729-4742. https://doi.org/10.1109/TIA.2015.2458954, (2015).
[4] Beltran B., Benbouzid M. E., and Ahmed-Ali T., Second-Order Sliding Mode Control of a Doubly Fed Induction Generator Driven Wind Turbine, IEEE Transactions on Energy Conversion, Vol. 27, N°. 2, June 2012, 0885-8969/$31.00 © 2012 IEEE.
[5] Wenjing Zhou, Modeling, Control and Optimization of a Hydropower Plant, University College of Southeast Norway Faculty of Technology, Natural Sciences and Maritime Sciences, PhD dissertation in Process, Energy and Automation Engineering, Doctoral dissertation no. 33 2017.
[6] Moussa O., Benguesmia H., Abdessemed R., Benaggoune S., High-order sliding mode control of a grid-connected brushless doubly fed induction generator, International Conference on Mechanics and Energy, December 19-21, 2019, Monastir, Tunisia ICME'2019.
[7] Boubzizi S., Abid H,, El hajjaji A., and Chaabane M,, Comparative study of three types of controllers for DFIG in wind energy conversion system, Springer, Protection and Control of Modern Power Systems, Protection and Control of Modern Power Systems (2018) 3:21 https://doi.org/10.1186/s41601-018-0096-y.
[8] Hao C., David N., and Dionysios C., Aliprantis C., Analysis of Permanent-Magnet Synchronous Generator with Vienna Rectifier for Wind Energy Conversion System, IEEE Transactions on Sustainable Energy, Vol. 4, N°. 1, January 2013. 1949-3029/$31.00 © 2012 IEEE.
[9] Berkani A., Negadi K., Allaoui T., Marignetti F., Sliding mode control of wind energy conversion system using dual star synchronous machine and three level converter, Tecnica Italiana-Italian Journal of Engineering Science, 63(2-4): 243-250. https://doi.org/10.18280/ti-ijes.632-418, (2019). 10.1177/0309524X17723202journals.sagepub.com/home/wie, 2018.
[10] Jain A., Shankar S., and Vanitha V., Power Generation using Permanent Magnet Synchronous Generator (PMSG) Based Variable Speed", Wind Energy Conversion System (WECS): An Overview, Journal of Green Engineering, Vol. 7 4, 477–504. doi: 10.13052/jge1904-4720.742, 27 March 2018.
[11] Meghni B., Dib D., Taher Azar A,, A second-order sliding mode and fuzzy logic control to optimal energy management in wind turbine with battery storage, Springer, Neural Computing & Applications, Vol 2 N°8 , November 2015, DOI 10.1007/s00521-015-2161-z.
[12] Krim Y., Abbes D., Krim S. and Mimouni M. F., Classical vector, first-order sliding mode and high-order sliding-mode control for a grid-connected variable speed wind energy conversion system: A comparative study, Wind Engineering 2018, Vol. 42(1) 16–37 © The Author(s) 2017 Reprints and permissions: sagepub.co.uk/journals Permissions. nav DOI: 10.1177/0309524X17723202 journals.sagepub.com/home/wie, 2018.
[13] Bouzaini K., Ben Slama S., Adnane C., Higher Order Sliding mode control For PMSG In Wind power Conversion System, Proceedings of 2016 4th International Conference on Control Engineering & Information Technology (CEIT-2016) Tunisia, Hammamet- December, 16-18, 2016, 978-1-5090-1055-4 © 2016 IEEE.
[14] Xinyi L., Laghrouche S., Harmouche M., Fellag R., Wack M., Super Twisting Sliding Mode MPPT Control of an IM based Wind Energy Conversion System, 978-1-4673-6673-1/15/$31.00 c 2015 IEEE.